# Soldering & Surface Mount Technology

Solder joint imagery compressing and recovery based on compressive sensing

Huihuang Zhao Yaonan Wang Zhijun Qiao Bin Fu

# Solder joint imagery compressing and recovery based on compressive sensing

*Huihuang Zhao*
College of Electrical and Information Engineering, Hunan University, ChangSha, China and Department of Computer Science, HengYang Normal University, HengYang, China

*Yaonan Wang*
College of Electrical and Information Engineering, Hunan University, ChangSha, China, and

*Zhijun Qiao and Bin Fu*
Department of Mathematics, University of Texas-Pan American, Texas, USA

**Abstract**

**Purpose** – The purpose of this paper is to develop an improved compressive sensing algorithm for solder joint imagery compressing and recovery. The improved algorithm can improve the performance in terms of peak signal to noise ratio (PSNR) of solder joint imagery recovery.

**Design/methodology/approach** – Unlike the traditional method, at first, the image was transformed into a sparse signal by discrete cosine transform; then the solder joint image was divided into blocks, and each image block was transformed into a one-dimensional data vector. At last, a block compressive sampling matching pursuit was proposed, and the proposed algorithm with different block sizes was used in recovering the solder joint imagery.

**Findings** – The experiments showed that the proposed algorithm could achieve the best results on PSNR when compared to other methods such as the orthogonal matching pursuit algorithm, greedy basis pursuit algorithm, subspace pursuit algorithm and compressive sampling matching pursuit algorithm. When the block size was $16 \times 16$, the proposed algorithm could obtain better results than when the block size was $8 \times 8$ and $4 \times 4$.

**Practical implications** – The paper provides a methodology for solder joint imagery compressing and recovery, and the proposed algorithm can also be used in other image compressing and recovery applications.

**Originality/value** – According to the compressed sensing (CS) theory, a sparse or compressible signal can be represented by a fewer number of bases than those required by the Nyquist theorem. The findings provide fundamental guidelines to improve performance in image compressing and recovery based on compressive sensing.

**Keywords** Assembly, Solder joints, Solder, Pin-in-paste

**Paper type** Research paper



## 1. Introduction

Compressed sensing (CS) is a sampling paradigm that provides the signal compression at a rate significantly lower than the Nyquist rate. Based on the CS theory, a sparse or compressible signal can be represented by a smaller number of bases than those required by the Nyquist theorem when it is mapped to the space with bases incoherent to the sparse data space (Donoho, 2006; Donoho *et al.*, 2006). The contents of most references are about imagery and raw data compressing and reconstruction based on the CS theory. CS has been successfully applied to magnetic resonance imaging (Lustig *et al.*, 2007), with consistent benefits in a clinical setting (Vasanawala *et al.*, 2010). In a study by Jørgensen *et al.* (2012), an iterative image reconstruction method in X-ray computed tomography (CT) was proposed based on compressive sensing (CS). Bhattacharya *et al.* (2007) proposes a new method of fast encoding for synthetic aperture radar (SAR) raw data by using the CS theory to complete SAR raw data compressing and reconstruction.

Nowadays, surface mount technology (SMT) components are widely used in the electronics industry. To detect surface-related defects such as pseudo solder, which is not a hidden open joint (Wu and Zhang, 2011), insufficient solder, component shift, wrong component use and tombstoning (Janoczki *et al.*, 2010), automatic inspection technologies, such as automatic optical inspection (AOI) and X-ray inspection, have been applied to SMT-based production and proved to be a useful supplement to circuit and functional testing (Hongwei *et al.*, 2011; Benedek *et al.*, 2013). To improve the inspection rate of defects, some image processing technologies, such as image compression, image enhancing and image filtering are used in AOI and SPI (Xiong *et al.*, 2012). Usually, wavelet transform and wavelet package transform are used in image compression (Karami *et al.*, 2012; Bayazit, 2011). Due to the steadily increasing resolution of the image acquisition platforms, the amount of image data produced is now constrained by storage capabilities and the slow

The current issue and full text archive of this journal is available at **www.emeraldinsight.com/0954-0911.htm**

Emerald

Soldering & Surface Mount Technology
26/3 (2014) 129–138

[ISSN 0954-0911]
[DOI 10.1108/SSMT-09-2013-0024]

The authors appreciate the careful comments of the anonymous reviewers. This work was supported by Key Construction Disciplines of the Hunan Province during the 12th Five-Year Plan period.

inspection speed (Wu *et al.*, 2013). Also, CS can be used in SMT, such as solder joint inspection, solder joint image processing and so on. There are few references about solder joint imagery data compressing and reconstruction based on the CS theory. In this paper, solder joint imagery data compressing and reconstruction based on CS have been studied.

This paper is organized as follows. In Section 2, the CS theory is presented. The signal recovery algorithms are presented in Section 3, and then some CS recovery algorithms are described in detail. The methodology of this paper and the block compressive sampling matching pursuit (CoSaMP) algorithm are presented in Section 4. Experimental results were obtained with the proposed method using solder images in Section 5. Finally, the conclusions are summarized at the end of this paper.

## 2. CS theory

### 2.1 Compressed sensing

CS is based on the assumption of the sparse property of a signal and incoherency between the bases of sparse domain and the bases of measurement vectors. CS has three major steps:

1 the construction of $k$-sparse representation;
2 the compression; and
3 the reconstruction.

The first step is the construction of $k$-sparse representation, where $k$ is the number of the non-zero entries of the sparse signal. Most natural signals can be made sparse by applying orthogonal transforms such as wavelet transform, fast Fourier transform and discrete cosine transform (DCT). This step is represented as (Candes and Wakin, 2008):

$$s = \Psi^T x \tag{1}$$

where $x$ is an $N$-dimensional non-sparse signal, $s$ is a weighted $N$-dimensional vector (sparse signal with $k$ non-zero elements) and $\Psi$ is an $N \times N$ orthogonal basis matrix. The second step is compression. In this step, the random measurement matrix is applied to the sparse signal according to the following equation:

$$y = \Phi s = \Phi \Psi^T x \tag{2}$$

where $\Phi$ is an $M \times N$ random measurement matrix ($M < N$).

Let $M$ be the number of measurements (the row dimension of $y$) sufficient for a high probability of successful reconstruction, and $M$ is determined by:

$$M \geq C\mu^2(\Phi, \Psi) k \log N \tag{3}$$

For some positive constant $C$, $\mu(\Phi, \Psi)$ is the coherence between $\Phi$ and $\Psi$ and is defined by:

$$\mu(\Phi, \Psi) = \sqrt{N} \max_{i,j} |<\phi_i, \psi_j>| \tag{4}$$

If the elements in $\phi$ and $\psi$ are correlated, the coherence is large. Otherwise, it is small. From linear algebra, it is known that $\mu(\Phi, \Psi) \in [1, \sqrt{N}]$.

### 2.2 Reconstruction method

Successful reconstruction depends on the measurement matrix $\Phi$ that complies with restricted isometry property (RIP). RIP is defined as follows (Cai and Wang, 2011):

$$(1 - \delta_k)||s||_2^2 \leq ||\Phi s||_2^2 \leq (1 + \delta_k)||s||_2^2 \tag{5}$$

where $||\,||_2$ defines the $l_2$ norm and $\delta_k$ is the $k$-restricted isometry constant of a matrix $\Phi$. RIP is used to ensure that all subsets of $k$ columns taken from $\Phi$ are nearly orthogonal. It should be noted that $\Phi$ has more columns than rows; thus, $\Phi$ cannot be exactly orthogonal.

The reconstruction is the optimization problem to solve (2). In (2), when $\Psi$ is an identity matrix. The following equation is the reconstruction problem used in this study:

$$\arg\max_x \|x\|_0 \ s.t.\ y = \Phi x \tag{6}$$

## 3. Signal recovery algorithm

The major algorithmic challenge in compressive sampling is to approximate a signal, given a vector of samples. The literature describes a huge number of approaches to solving this problem. They fall into three rough categories:

1 *Convex optimization:* These techniques solve a convex program whose minimizer is known to approximate the target signal. Many algorithms have been proposed to complete the optimization, including basis pursuit (BP) (Bazerque and Giannakis, 2013), projected gradient methods (Figueiredo *et al.*, 2007) and iterative hard thresholding (Blumensath and Davies, 2009).
2 *Iterative greedy algorithms:* These methods build up an approximation one step at a time by making locally optimal choices at each step. Examples include matching pursuit (MP) (Tropp and Gilbert, 2007), orthogonal matching pursuit (OMP), regularized OMP (Needell *et al.*, 2009), stage-wise OMP (StOMP) (D. L. Donoho *et al.*, 2012) and CoSaMP (Needell *et al.*, 2010).
3 *Combinatorial algorithms:* These methods acquire highly structured samples of the signal that support rapid reconstruction via group testing. This class includes Fourier sampling (A. Gilbert *et al.*, 2007), HHS pursuit (Gilbert *et al.*, 2005) and Iwen (Iwen, 2008).

Here, attention is focused on the OMP algorithm, greedy basis pursuit (GBP) algorithm, subspace pursuit (SP) algorithm and CoSaMP algorithm (Davenport *et al.*, 2013).

### 3.1 Orthogonal matching pursuit

OMP is an iterative greedy algorithm that selects, at each step, the column of measurement matrix which is most correlated with the current residuals. This column is then added into the set of selected columns. The algorithm updates the residuals by projecting the observation onto the linear subspace spanned by the columns that have already been selected, and the algorithm then iterates. Compared with other alternative methods, a major advantage of the OMP is its simplicity and fast implementation. The following lists the steps of the OMP algorithm.

Algorithm 1. OMP recovery algorithm

Input:
An $m \times N$ measurement matrix $\Phi$, an $m$-dimensional data vector $v$ and the sparsity level $s$ of the ideal signal.

Initialization:
Initialize the residual $r_0 = v$, the index set $\Lambda_0 = \varnothing$ and the iteration counter $t = 1$.

Procedure:

1 Find the index $\lambda_t$ that solves the easy optimization problem:

$$\lambda_t = \arg\max_{j=1,\dots d} |<r_{t-1}, \varphi_j>|$$

If the maximum occurs for multiple indices, break the tie deterministically.

2 Augment the index set and the matrix of chosen atoms: $\Lambda_t = \Lambda_{t-1} \cup \{\lambda_t\}$ and $\Phi_t = [\Phi_{t-1}\ \varphi\lambda_t]$. We use the convention that $\Phi_0$ is an empty matrix.

3 Solve a least squares problem to obtain a new signal estimate:

$$x_t = \arg\min_x \|v - \Phi_t x\|_2$$

4 Calculate the new approximation of the data and the new residual:

$$a_t = \Phi_t x_t; r_t = v - a_t$$

5 Increment $t$ and return to step (2) if $t < m$ or $r_{t-1} = 0$.

6 The estimate $\hat{s}$ for the ideal signal has non-zero indices at the components listed in $\Lambda_m$. The value of the estimate $\hat{s}$ in component $\lambda_j$ equals the $j$th component of $x_t$.

End

Output:

An estimate $\hat{s}$ in $M \times d$ matrix $R^d$ for the ideal signal, a set $\Lambda_m$ containing $m$ elements from $\{1 \dots, d\}$ and an $N$-dimensional approximation $a_m$ of the data vector $v$.

### 3.2 Greedy basis pursuit

GBP is rooted in computational geometry and exploits an equivalence between minimizing the $l^1$-norm of the representation coefficients and determining the intersection of the signal with the convex hull of the dictionary. GBP unifies the different advantages of previous algorithms. It builds up representations, sequentially selecting atoms. The following lists the steps of the GBP algorithm.

Algorithm 2: CS recovery using GBP

Input:

A signal $x \in R^d$, a dictionary $D = \{\psi_i\}_i^n = 1$ and a threshold $\varepsilon \geq 0$; a representation of $x$, consisting of a set of indices $I \subseteq \{1, \dots n\}$ and a set of coefficients $A = \{\alpha_i\} i \in I$, such that $x - \sum_{i \in I} \alpha_i \psi_i < \varepsilon$.

Procedure:

Initialize:

1 Select the first atom:

$$k = \arg\max_{i \in \{1, \dots n\}} < x, \psi_i>$$

2 Compute the initial approximation:

$$\alpha_k = <x, \psi_k>, I^{(0)} = \{k\}, A^{(0)} = \{\alpha_k\};$$

3 Initialize the biorthogonal system:

$$\Psi^{\perp} = \{\psi_k\}$$

4 Initialize the hyperplane:

$$\tilde{x}^{(0)} = \alpha_k \psi_k, n = x/\|x\|, r = x - \tilde{x}$$

Repeat until:

1 Compute the center and plane of rotation:

$$\tilde{x}_H = (<\psi_i, n> / <\tilde{x}, n>)\tilde{x}, \textit{for any } i \in I$$

$$v = (r - <r, n> n/\|r - <r, n> n)\|$$

2 Project atoms into the $n - v$-plane and select the next atom:

$$k = \arg\min_{i \in \{1, \dots n\}} \tan^{-1} \frac{<\psi_i - \tilde{x}_H, n>}{<\psi_i - \tilde{x}_H, v>}$$

3 Compute the new representation and update the biorthogonal system:

$$\{I, A, \Psi^{\perp}\} = AddAtom(x, I, A, \psi_k, \Psi^{\perp}).$$

4 Discard any extraneous atoms while:

$$\exists\, a_i \leq 0, i \in I \textit{ do}$$

$$\{I, A, \Psi^{\perp}\} = SubstractAtom(x, I, A, \psi_j, \Psi^{\perp})$$

5 Update the hyperplane parameters:

$$\tilde{x} = \sum_{i \in I} \alpha_i \psi_i;$$

$$n = \frac{-<\psi_k - \tilde{x}_H, n> v + <\psi_k - \tilde{x}_H, v> n}{\|-<\psi_k - \tilde{x}_H, n> v + <\psi_k - \tilde{x}_H, v> n\|};$$

$$r = x - \tilde{x}$$

### 3.3 Compressive sampling matching pursuit

CoSaMP is at heart a greedy pursuit algorithm. It is initialized with a trivial signal approximation, which means that the initial residual equals the unknown target signal. During each iteration, CoSaMP performs five major steps, including identification, support merger, estimation, pruning and sample update. These steps are repeated until the halting criterion is triggered.

The following lists the steps of the CoSaMP algorithm.

Algorithm 3. CoSaMP recovery algorithm.

Input:

Sampling matrix $\Phi$, sample vector $u$ and sparsity level $K$.

Procedure:

Initialize:

$a^0 = 0$; $v = u$; $n = 0$; $v$ is current samples and $n$ is an iteration counter.

Repeat:

1 $n = n + 1$, form signal proxy, $y = \Phi^* v$, $\Phi^*$ is the Hermitian transpose of $\Phi$;

2 Identify large components:

$$\Omega = \mathrm{supp}(y_n);$$

3 Merge support:

$$T = \Omega \cup \mathrm{supp}(a^{n-1});$$

4 Signal estimation by least squares: $b|_T = \Phi_T^\dagger u$, $b|_{T^c} = 0$, $\Phi^\dagger$ is the pseudo-inverse of $\Phi$ such that $\Phi^\dagger = (\Phi^*\Phi)^{-1}\Phi^*$; $T^C$ indicates the compliment of set T; and $b|_T$ indicates the vector b is restricted by only the elements given in T.

5 Prune to obtain next approximation: $a^n = b_k$;

6 Update current samples: $v = u - \Phi a^n$; until halting criterion is true.

Output:

A $K$-sparse approximation $a$ of the target signal.

### 3.4 Subspace pursuit

The main difference between subspace pursuit (SP) and CoSaMP is the manner of adding new candidates. More precisely, SP only adds K new candidates in each iteration, while CoSaMP adds 2K, which makes the SP computationally more efficient but the underlying analysis more complex. The following lists the steps of the SP algorithm.

Algorithm 4: CS recovery using SP

Input:

The CS observation $y$, a measurement matrix $\Phi \in R^{m \times n}$, a signal sparse transform matrix $\Psi \in R^{n \times n}$; sample vector $u$, sparsity level $K$.

Procedure:

Initialization:

$T^0$ = {K indices corresponding to the largest magnitude entries in the vector $\Phi^* y$}; $y_r^0 = resid(y, \Phi_{T0})$.

Iteration: At the $l^{th}$ iteration, go through the following steps:

1 $\widetilde{T}^l = \widetilde{T}^{l-1} \cup$ {K indices corresponding to the largest magnitude entries in the vector $\Phi^* y_r^{l-1}$};

2 Set $x_p = \Phi_{\widetilde{T}l}^\dagger y$, where $\Phi_{\widetilde{T}l}^\dagger = (\Phi_{\widetilde{T}l}^* \Phi_{\widetilde{T}l})^{-1} \Phi_{\widetilde{T}l}^*$;m,

3 $T^l$ = {K indices corresponding to the largest elements of $x_p$};

4 $y_r^l = resid(y, \Phi_{Tc})$;

5 If $||y_r^l||_2 > ||y_r^{l-1}||_2$, let $T^l = T^{l-1}$ and quit the iteration.

Output:

The estimated signal $\hat{x}$, satisfying $\hat{x}_{\{1,2...,N\} - T^l} = 0$ and $\hat{x}_{T^l} = \Phi_{T^l}^\dagger y$.

## 4. Reconstruction algorithms for block compressed sensing

### 4.1 Block compressed sensing

An $N_1 \times N_2$ image is divided into small blocks with a size of $n_1 \times n_2$. Let $f_i$ represent the vectorized signal of the $i$-th block through raster scanning, $i = 1, 2$ [. . .] $n$ and $n = N_1N_2/n_1n_2$. An $m$-dimensional sampled vector $y_b$ can be obtained through the following linear transformation (Eldar *et al.*, 2010):

$$y_b = \Phi_B f_i \tag{7}$$

where $f_i$ is an $n_1n_2$-dimensional vector, $\Phi_B$ is an $m \times n_1n_2$ measurement matrix, $m \ll n_1n_2$. Note that block CS is memory efficient, as we just need to store an $m \times n_1n_2$ Gaussian ensemble $\Phi_B$, rather than a full $M \times N_1N_2$ (i.e. $nm \times n_1n_2$) one. Small requires less memory in storage and faster implementation, while large offers better reconstruction performance.

The main advantages of block-based CS can be summarized as follows:

- The measurement operator can easily be stored and implemented through a random under-sampled filter bank.
- Block-based measurement is more advantageous for real-time applications, as the encoder does not need to send the sampled data until the whole image is measured.
- Because each block is processed independently the initial solution can be obtained and the reconstruction process is substantially sped up.

### 4.2 Reconstruction algorithm

It can be seen from the introduction of the CoSaMP algorithm above that the algorithm is initialized with a trivial signal approximation, which means that the initial residual equals the unknown target signal. During each iteration, CoSaMP performs five major steps:

1 *Identification.* The algorithm forms a proxy of the residual from the current samples and locates the largest components of the proxy.

2 *Support merger.* The set of newly identified components is united with the set of components that appear in the current approximation.

3 *Estimation.* The algorithm solves a least squares problem to approximate the target signal on the merged set of components.

4 *Pruning.* The algorithm produces a new approximation by retaining only the largest entries in this least squares signal approximation.

5 *Sample update.* Finally, the samples are updated so that they reflect the residual, the part of the signal that has not been approximated.

These steps are repeated until the halting criterion is triggered.

In his study, an improved CoSaMP algorithm was used for signal recovery based on block compressing sensing. The detailed algorithm is shown as follows.

Algorithm 5. Block CoSaMP algorithm

Input:

1 An image can be divided into some small blocks of a size $n_i \times m_i$, sample rate $w$ ($w \in (0, 1]$);

2 The sparsity level $k$ of the block images;

3 An $M \times N$ measurement matrix $\Phi$, $N = n^*m$, $M = N^*w$.

Output:

An estimate $\hat{x}$ of an image x

For each block $n_i \times m_i$ image procedure:

Initialization:

i Transform each $n_i \times m_i$ image block into an $(n_i^* m_i) \times 1$ data vector $y$;

ii $\hat{x}_{-1} = 0$ ($\hat{x}_{\mathcal{J}}$ is the estimate at the $\mathcal{J}$th iteration); and

iii $r = y$ (the current residual).

Procedure:

Loop until convergence

i Compute the current error:

$$e^i = \Phi^{i*} r^{\,i}$$

ii Compute the best $2k$ support set of the error (index set):

$$\Omega^i = e^i_{2k}$$

iii Merge the strongest support sets:

$$T^{\,i} = \Omega^i \cup \mathrm{supp}(\hat{x}^i_{\mathcal{J}-1})$$

iv Perform a least squares signal estimation (Johnson *et al.*, 2012):

$$b^i|_{Ti} = \Phi^{i\dagger}{}_{|\,Ti}\, y,\; b^i|_{TiC} = 0.$$

v Prune

$$\hat{x}^i_{\mathcal{J}}$$

and compute $r^i$ for next round:

$$\hat{x}^i_{\mathcal{J}} = b^i{}_k;\; r^{\,i} = y^i - \Phi^i \hat{x}^i_{\mathcal{J}}.$$

vi Each

$$\hat{x}^i_{\mathcal{J}}$$

consists of $\hat{x}$.

End

## 5. Experiment

To evaluate the quality of the reconstructed results, the mean square error and peak signal noise ratio (PSNR) can be utilized. They are defined as follows (Huynh-Thu and Ghanbari, 2008);

$$\frac{1}{M \times N} \sum_{i=1}^{M} \sum_{j=1}^{N} (\hat{f}(i,j) - f(i,j))^2 \tag{8}$$

$$\mathrm{PSNR} = 10\log_{10}\left(\frac{255^2}{MSE}\right) \tag{9}$$

where M and N are the image dimensions, $\hat{f}$ is the de-noised image and $f$ is the original noiseless image. In this study, the PSNR was used to compare the experimental results.

An original gull-wing lead solder joint image was used as a test image in Figure 1(a) (size 256 × 256). The sparse transform DCT matrix and sparse image are shown in Figure 1(b,c).

The reconstruction result based on conventional CS with matrix R's rows M = 180 can be seen in Figure 2(b-e), and the reconstruction result based on block CS with sample rate 0.7

**Figure 1** Original image and sparse image

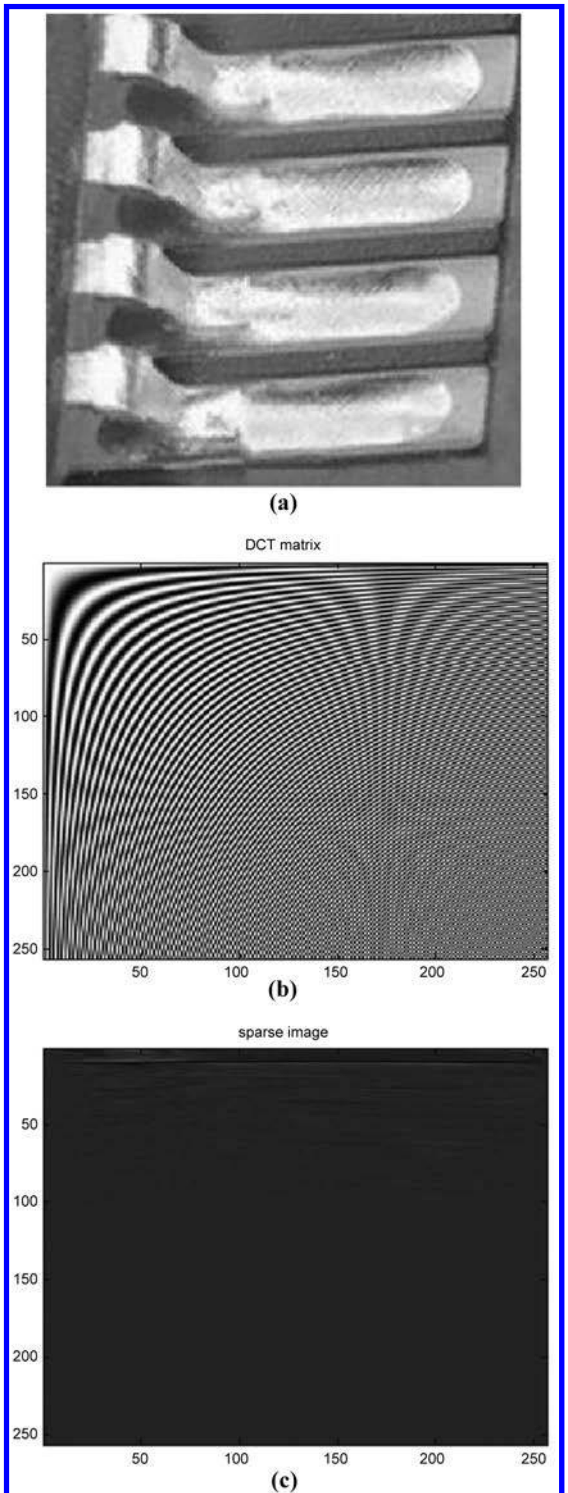


**Notes:** (a) Original image; (b) Sparse transform DCT matrix; (c) Sparse image

(M/N ≈ 0.7) and block sizes 4 × 4, 8 × 8 and 16 × 16 can be seen in Figure 2(f-h).

The reconstruction result based on conventional CS with matrix R's rows M = 230 can be seen in Figure 3(b-e), and the

Soldering & Surface Mount Technology
Volume 26 · Number 3 · 2014 · 129–138

**Figure 2** Reconstruction results

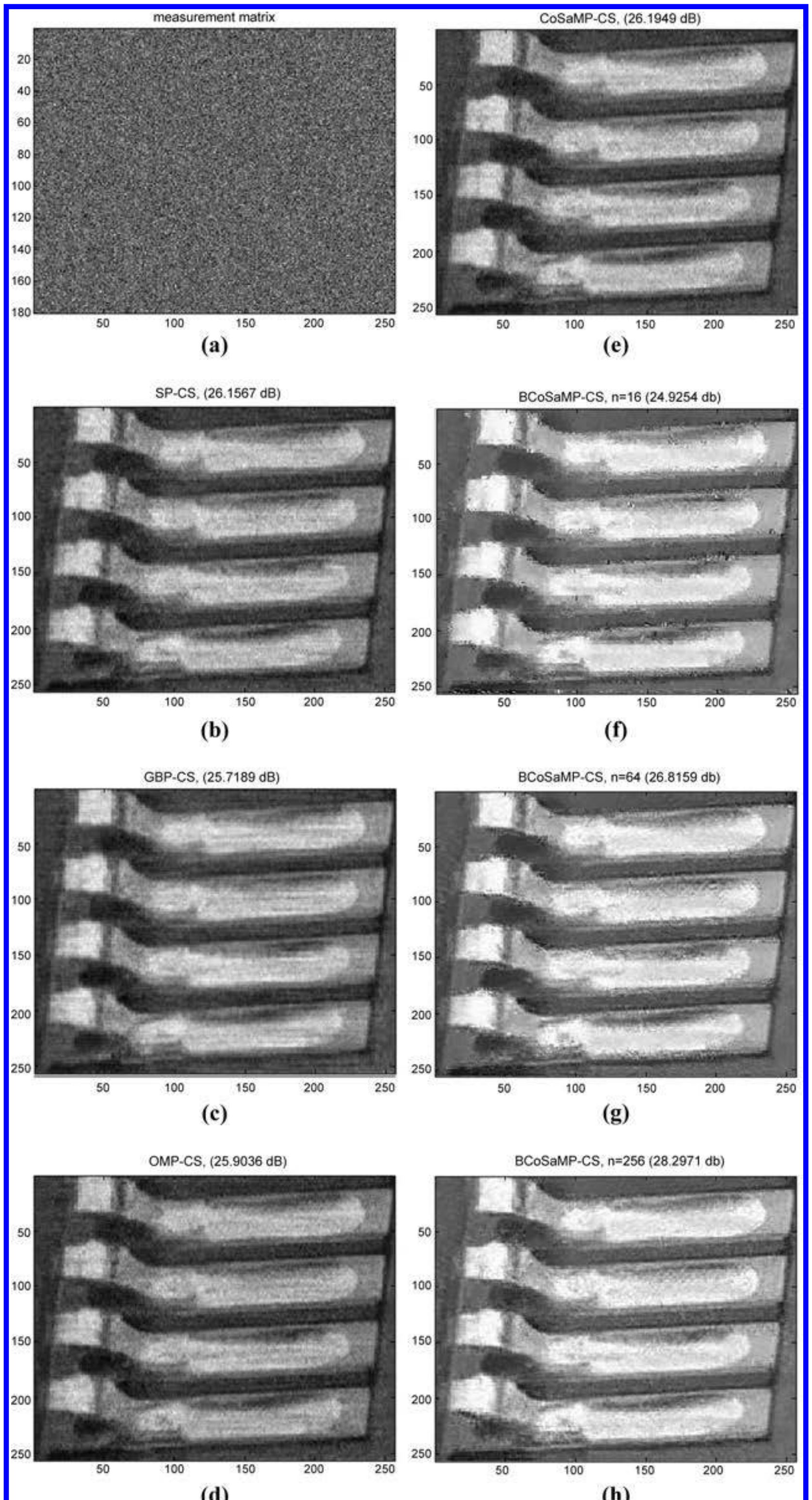


**Notes:** Reconstructed results by using the different methods: (a) measurement matrix in image reconstruction; (b) result by SP algorithm; (c) result by GBP algorithm; (d) result by OMP algorithm; (e) result by CoSaMP algorithm; (f) result by block-CoSaMP algorithm ($N = 16$); (g) result by block-CoSaMP algorithm ($N = 64$); (h) result by block-CoSaMP algorithm ($N = 256$)

**Figure 3** Reconstruction results

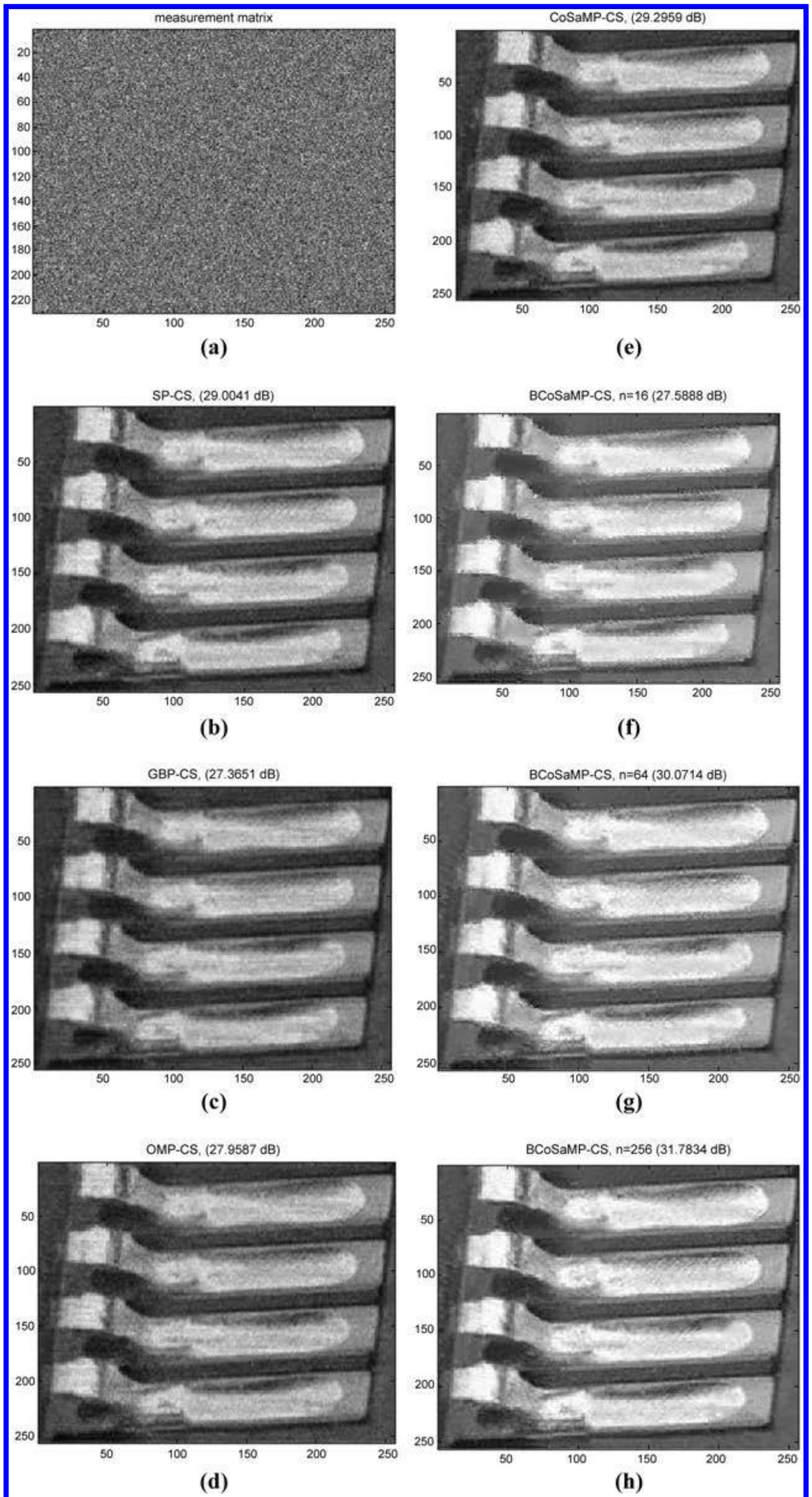


**Notes:** Reconstructed results by using the different methods: (a) measurement matrix in image reconstruction; (b) result by SP algorithm; (c) result by GBP algorithm; (d) result by OMP algorithm; (e) result by CoSaMP algorithm; (f) result by block-CoSaMP algorithm ($N = 16$); (g) result by block-CoSaMP algorithm ($N = 64$); (h) result by block-CoSaMP algorithm ($N = 256$)

**Table I.** Quantization comparison of reconstructed results

| M (M/N) Methods | 180 (0.70) | 190 (0.74) | 200 (0.78) | 210 (0.82) | 220 (0.86) | 230 (0.90) | 240 (0.94) | 250 (0.98) |
|---|---|---|---|---|---|---|---|---|
| SP_CS | 26.1567 | 27.0200 | 27.2385 | 27.7911 | 28.5089 | 29.0041 | 29.3168 | 29.7900 |
| GBP_CS | 25.7189 | 25.7793 | 26.4902 | 26.7375 | 27.1526 | 27.3651 | 27.7130 | 27.8708 |
| OMP_CS | 25.9036 | 26.3989 | 26.7542 | 27.2056 | 27.5076 | 27.9587 | 28.2425 | 28.7103 |
| CoSaMP_CS | 26.1949 | 27.0296 | 27.5797 | 28.2773 | 29.0022 | 29.2959 | 30.0350 | 30.3546 |
| Block CoSaMP_CS (N = 16) | 24.9254 | 25.9316 | 25.8103 | 26.8031 | 27.4728 | 27.5888 | 27.9073 | 29.1033 |
| Block CoSaMP_CS (N = 64) | 26.8159 | 27.4830 | 28.2680 | 28.6433 | 29.2425 | 30.0714 | 30.8152 | 31.0331 |
| Block CoSaMP_CS (N = 256) | 28.2971 | 29.1184 | 29.8828 | 30.3825 | 31.2553 | 31.7834 | 32.4744 | 32.8773 |

**Figure 4** Quantization comparisons of reconstructed results with different block size

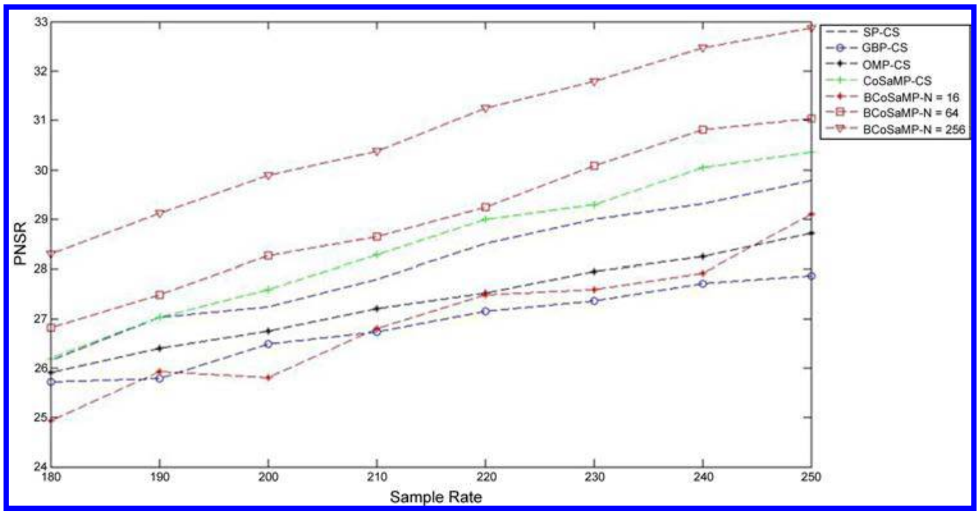




reconstruction result based on block CS with sample rate 0.9 (M/N ≈ 0.9) and block size 4 × 4, 8 × 8 and 16 × 16 can be seen in Figure 3(f-h).

It can seen by comparing Figure 3(f-h) that the method reported here can obtain better results in PSNR than the results obtained from methods based on conventional CS. The results for varying sample rates are summarized in Table I.

From Table I, it can be seen that the PSNR of the reconstructed results is improved. The new method reported in this paper can obtain better results than those based on conventional CS. The quantization comparison of reconstructed results with different block size can be seen in Figure 4.

As can be seen from Figure 4, the method when block size is 8 × 8 ($N$ = 64) can obtain better results than other traditional methods. During the improved methods, when the block size is 16 × 16 ($N$ = 256), the best results were obtained.

## 6. Conclusion

This paper has focused on the development of compressing and reconstruction methods for solder joint imagery. There are many algorithms in compressive sampling that have been used to approximate a signal, given a vector of samples. Among them, CoSaMP achieves good performance on PNSR. Solder joint image were divided into some blocks, and an image reconstruction method was proposed based on block compressing sensing with the CoSaMP algorithm. The performance of the proposed approach has been shown and compared with different block sizes. The main advantages of block CoSaMP are as follows:

- Measurement operator can easily be stored and implemented through a random under-sampled filter bank.
- Block-based measurement is more advantageous for real-time applications.
- The proposed algorithm can be obtained and can achieve the best result on PNSR than other methods.
- The block CoSaMP algorithm when block size is 16 × 16 can obtain better results than when the block size is 8 × 8 and 4 × 4.

In future studies, the relationship between the size of block and recovery performance will be researched, and the speed of the proposed algorithm will also be considered.

## References

Bayazit, U. (2011), "Adaptive spectral transform for wavelet-based color image compression", *IEEE Transactions on Circuits and Systems for Video Technology*, Vol. 21 No. 7, pp. 983-992.

Bazerque, J.A. and Giannakis, G.B. (2013), "Nonparametric basis pursuit via sparse kernel-based learning", *IEEE Signal Processing Magazine*, Vol. 30 No. 4, pp. 112-125.

Benedek, C.S., Krammer, O., Janóczki, M. and Jakab, L. (2013), "Solder Paste Scooping Detection by Multi-Level Visual Inspection of Printed Circuit Boards", *IEEE Transactions on Industrial Electronics*, Vol. 60 No. 6, pp. 2318-2331.

Bhattacharya, S., Blumensath, T., Mulgrew, B. and Davies, M. (2007), "Fast encoding of synthetic aperture radar raw data using compressed sensing", *2007 IEEE/SP 14th Workshop on Statistical Signal Processing*, *Madison, WI*, *26-29 August*, pp. 448-452.

Blumensath, T. and Davies, M. (2009), "Iterative hard thresholding for compressive sensing", *Applied and Computational Harmonic Analusis*, Vol. 27 No. 3, pp. 265-274.

Cai, T.T. and Wang, L. (2011), "Orthogonal matching pursuit for sparse signal recovery with noise", *IEEE Transaction on Information Theory*, Vol. 57 No. 7, pp. 4680-4688.

Candes, E.J. and Wakin, M.B. (2008), "An introduction to compressive sampling", *IEEE Signal Processing Magazine*, Vol. 25 No. 2, pp. 21-30.

Davenport, M.A., Needell, D. and Wakin, M.B. (2013), "Signal space CoSaMP for sparse recovery with redundant dictionaries", *IEEE Transactions on Information Theory*, Vol. 9 No. 9, pp. 1-18.

Donoho, D.L. (2006), "Compressed sensing", *IEEE Transactions on Information Theory*, Vol. 52 No. 4, pp. 1289-1306.

Donoho, D.L., Elad, M. and Temlyakov, V. (2006), "Stable recovery of sparse overcomplete representations in the presence of noise", *IEEE Transactions on Information Theory*, Vol. 52 No. 1, pp. 6-18.

Donoho, D.L., Tsaig, Y., Drori, I. and Starck, J.-L. (2012), "Sparse solution of underdetermined systems of linear equations by stagewise orthogonal matching pursuit", *IEEE Transactions on Information Theory*, Vol. 58 No. 2, pp. 1094-1121.

Eldar, Y.C., Kuppinger, P. and Bolcskei, H. (2010), "Compressed sensing of block-sparse signals: uncertainty relations and efficient recovery", *IEEE Transactions on Signal Processing*, Vol. 58 No. 6, pp. 3042-3054.

Figueiredo, M.A.T., Nowak, R.D. and Wright, S.J. (2007), "Gradient projection for sparse reconstruction: Application to compressed sensing and other inverse problems", *IEEE J. Selected Topics in Signal Processing: Special Issue on Convex Optimization Methods for Signal Processing*, Vol. 1 No. 4, pp. 586-598.

Gilbert, A.C., Muthukrishnan, S. and Strauss, M.J. (2005), "Improved time bounds for near-optimal sparse Fourier representation via sampling", in *Proceedings of SPIE Wavelets, XI, San Diego, CA*.

Gilbert, A., Strauss, M., Tropp, J. and Vershynin, R. (2007), "One sketch for all: fast algorithms for compressed sensing", in *Proceeding 2007 39th ACM Symposium Theory of Computing*, *San Diego*, *June*.

Hongwei, X., Xianmin, Z., Yongcong, K. and Gaofei, O. (2011), "Solder joint inspection method for chip component using improved AdaBoost and decision tree", *IEEE Transaction on components, Packaging and Manufacturing Technology*, Vol. 1 No. 12, pp. 218-227.

Huynh-Thu, Q. and Ghanbari, M. (2008), "Scope of validity of PSNR in image/video quality assessment", *Electronics Letters*, Vol. 44 No. 13, pp. 800-801.

Iwen, M. (2008), "A deterministic sub-linear time sparse Fourier algorithm via non-adaptive compressed sensing methods", *2008 in Proceeding ACM-SIAM Symposium on Discrete Algorithms (SODA)*, *San Francisco, CA*, *January*, pp. 20-29.

Janoczki, M., Borbiro, A., Nagy, S. and Jakab, L. (2010), "Illumination optimization for quasi-tombstone detection", *Micro and Nanosystems*, Vol. 2 No. 3, pp. 149-162.

Johnson, K.M., Block, W.F., Reeder, S.B. and Samsonov, A. (2012), "Improved least squares MR image reconstruction using estimates of k-Space data consistency", *Magnetic Resonance in Medicine*, Vol. 67 No. 6, pp. 1600-1608.

Jørgensen, J.H., Sidky, E.Y. and Pan, X. (2012), "Quantifying admissible undersampling for sparsity-exploiting iterative image reconstruction in X-ray CT", *IEEE Transactions on Medical Imaging*, Vol. 32 No. 2, pp. 460-473.

Karami, A., Yazdi, M. and Mercier, G. (2012), "Compression of hyperspectral images using discerete wavelet transform and tucker decomposition", *IEEE Journal of Selected Topics in Applied Earth Observations and Remote Sensing*, Vol. 5 No. 2, pp. 444-450.

Lustig, M., Donoho, D. and Pauly, J.M. (2007), "Sparse MRI: the application of compressed sensing for rapid MR imaging", *Magnetic Resonance in Medicine*, Vol. 58 No. 6, pp. 1182-1195.

Needell, D. and Tropp, J.A. (2010), "CoSaMP: iterative signal recovery from incomplete and inaccurate samples", *Communications of the ACM*, Vol. 53 No. 12, pp. 93-100.

Needell, D. and Vershynin, R. (2009), "Uniform uncertainty principle and signal recovery via regularized orthogonal matching pursuit", *Foundations of Computational Mathematics*, Vol. 9 No. 3, pp. 317-334.

Tropp, J.A. and Gilbert, A.C. (2007), "Signal recovery from random measurements via orthogonal matching pursuit", *IEEE Transaction on Information Theory*, Vol. 53 No. 12, pp. 4655-4666.

Vasanawala, S.S., Alley, M.T., Hargreaves, B.A., Barth, R.A., Pauly, J.M. and Lustig, M. (2010), "Improved pediatric MR imaging with compressed sensing", *Radiology*, Vol. 256 No. 2, pp. 607-616.

Wu, F. and Zhang, X. (2011), "Inspection of pseudo solders for lead-free solder joints in PCBs", *Optics and Precision Engineering*, Vol. 19 No. 3, pp. 697-702.

Wu, H., Zhang, X., Xie, H., Kuang, Y. and Ouyang, G. (2013), "Classification of solder joint using feature selection based on bayes and support vector machine", *IEEE Transactions on components Packaging and Manufacturing Technology*, Vol. 3 No. 3, pp. 516-522.

Xiong, G., Lu, J. and Wu, S. (2012), "New Automatic Optical Inspection System for PCB", *Proceedings of the 2012 International Conference on Electronics*, *Communications and Control*, pp. 1270-1273.

## About the authors

**Huihuang Zhao** received a PhD degree from the School of Mechano-Electronic Engineering, Xidian University, Xi'an,

China, in 2010. He is currently Assistant Professor in the Computer Science Department, Hengyang Normal University. His research interests include computer vision and surface mount technology. Huihuang Zhao is the corresponding author and can be contacted at: happyday.huihuang@gmail.com

**Wang Yaonan** received a PhD degree from Hunan University in 1994. He is Professor and Doctoral Supervisor in Hunan University and is the Dean of College of Electrical and Information Engineering. His research interests include intelligent control and pattern recognition.

**Zhijun Qiao** received a PhD degree from Fudan University in 1997. He is Professor of Mathematics in the Department of Mathematics, University of Texas-Pan American. His research interests include integrable systems, solitons, Image PDEs and analysis, mathematical model, compressive sensing and radar image reconstructions.

**Bin Fu** received a PhD degree from Yale University in 1998. He is Professor of Computer Science in the Department of Computer Science, University of Texas-Pan American. His research interests include bioinformatics algorithms and computational complexity theory.